Neoplasia 57 (2024) 101049

Contents lists available at ScienceDirect

Neoplasia

journal homepage: www.elsevier.com/locate/neo

Original Research

ELAVL1 regulates PD-L1 mRNA stability to disrupt the infiltration of CD4-positive T cells in prostate cancer

Zhonglin Cai [a,b,1], Xiuxia Zhai [c,d,1], Jidong Xu [a,1], Tianyu Hong [a,1], Kuo Yang [a], Shasha Min [a], Jianuo Du [a], Zhikang Cai [a,*****], Zhong Wang [a,****], Ming Shen [e,***], Di Wang [f,**], Yanting Shen [a,*]

[a] Department of Urology, Gongli Hospital of Shanghai Pudong New Area, Shanghai, China
[b] Department of Urology, Shanghai Ninth People's Hospital, Shanghai Jiaotong University School of Medicine, Shanghai, China
[c] School of Nursing, Peking University, Beijing, China
[d] Health Service Department of the Guard Bureau of the General Office of the Central Committee of the Communist Party of China, Beijing, China
[e] National Health Commission (NHC) Key Laboratory of Reproduction Regulation, Shanghai Institute for Biomedical and Pharmaceutical Technologies, Shanghai, China
[f] Center for bioinformatics, National Infrastructures for Translational Medicine, Institute of Clinical Medicine and Peking Union Medical College Hospital, Chinese Academy of Medical Sciences and Peking Union Medical College, Beijing, China

ARTICLE INFO

Keywords:
Prostate cancer
ELAVL1
Androgen receptor
m6A
Tumor immune

ABSTRACT

Prostate cancer (PCa) currently ranks second in male tumor mortality. Targeting immune checkpoint in tumor as immunotherapy is a new direction for tumor treatment. However, targeting PD-1/PD-L1 and CTLA4 to treat PCa has poor immunotherapeutic efficacy because PCa is known as a cold tumor. Understanding the mechanism of immunosuppression in PCa can promote the use of immunotherapy to treat PCa. ELAVL1 is highly expressed in many tumors, participates in almost all tumor biological activities and is an oncogene. ELAVL1 is also involved in the development and differentiation of T and B lymphocytes. However, the relationship between ELAVL1 and tumor immunity has not yet been reported. In recent years, ELAVL1 has been shown to regulate downstream targets in an m6A -dependent manner. PD-L1 has been shown to have m6A sites in multiple tumors that are regulated by m6A. In this study, ELAVL1 was highly expressed in PCa, and PCa with high ELAVL1 expression is immunosuppressive. Knocking down ELAVL1 reduced PD-L1 expression in PCa. Moreover, PD-L1 was shown to have an m6A site, and its m6A level was upregulated in PCa. ELAVL1 interacts with *PD-L1* mRNA and promotes *PD-L1* RNA stability via m6A, ultimately inhibiting the infiltration of CD4-positive T cells. In addition, androgen receptor (AR) was shown to be regulated with ELAVL1, and knocking down AR could also affect the expression of PD-L1. Therefore, ELAVL1 can directly or indirectly regulate the expression of PD-L1, thereby affecting the infiltration of CD4-positive T cells in PCa and ultimately leading to immune suppression.

Introduction

Prostate cancer (PCa) is a common tumor among elderly men, and it has become the second most common tumor in the world [1]. PCa mortality has become the second leading cause of cancer-related mortality in males [2]. Although there are currently many treatment methods for PCa, including radical prostatectomy, radiotherapy, androgen deprivation therapy, chemotherapy, and androgen receptor

* Corresponding author at: Department of Urology, Gongli Hospital of Shanghai Pudong New Area, 219 Miao Pu Road, Shanghai, 200135, China.
** Corresponding author at: Center for bioinformatics, National Infrastructures for Translational Medicine, Institute of Clinical Medicine and Peking Union Medical College Hospital, Chinese Academy of Medical Sciences and Peking Union Medical College, 1 Shuai Fu Yuan, Dongcheng District, Beijing 100005, China.
*** Corresponding author at: National Health Commission (NHC) Key Laboratory of Reproduction Regulation, Shanghai Institute for Biomedical and Pharmaceutical Technologies, Shanghai 200032, China.
**** Corresponding author at: Department of Urology, Gongli Hospital of Shanghai Pudong New Area, 219 Miao Pu Road, Shanghai, 200135, China.
***** Corresponding author at: Department of Urology, Gongli Hospital of Shanghai Pudong New Area, 219 Miao Pu Road, Shanghai, 200135, China.
E-mail addresses: 32955997@qq.com (Z. Cai), zhongwang2000@sina.com (Z. Wang), shenming711@163.com (M. Shen), wangdi0001@foxmail.com (D. Wang), shenyanting798@126.com (Y. Shen).
[1] Contributed equally.

https://doi.org/10.1016/j.neo.2024.101049
Received 25 July 2024; Received in revised form 17 August 2024; Accepted 28 August 2024

antagonists, tumor recurrence or progression to castration-resistant prostate cancer (CRPC) cannot be ignored. The progression to CRPC significantly increases the mortality rate of PCa, which is attributed to drug tolerance [3]. In recent years, tumor immunotherapy has opened up a new era in the treatment of tumors, providing a new means for cancer treatment. However, PCa immunotherapy often fails to achieve a satisfactory prognosis [4,5], and improving the results is critical for PCa immunotherapy.

PCa is considered a cold tumor due to its poor response to immune checkpoint inhibitors, including PD-1/PD-L1 and CTLA4 [6-8]. Accumulating evidence has shown that the tumor microenvironment of PCa is immunosuppressive, and the tumor itself has low immunogenicity [5, 9]. Further research has shown that the levels of antigen expression genes and antigen processing- and presentation-related genes are low, in PCa and there is a lack of recruitment and activation of cytotoxic T cells [10,11]. In addition, the infiltration of CD8+ T cells in PCa is very low [12]. These factors have led to the poor response of PCa to tumor immunotherapy. Reversing the immunosuppressive environment of PCa is critical to improving the effectiveness of tumor immunotherapy.

The reason why these hot tumors can respond to immunotherapy is because their growth depends on immune checkpoints, such as PD-L1 [13]. PD-L1 was the earliest discovered classic immune checkpoint, and inhibitors targeting PD-L1 have shown satisfactory therapeutic effects against multiple tumors [14-16]. Several studies have shown that inhibiting the expression of PD-L1 can promote the infiltration of immune cells in tumors, including bladder cancer and intrahepatic cholangiocarcinoma, and play a role in immune killing [17-19]. In recent years, the m6A modification has been found on PD-L1 mRNA and is regulated by the methylase METTL3, demethylase ALKBH5, and methylation binding protein YTHDF1 [17,18,20]. PD-L1 mRNA is regulated by altering RNA metabolic processes via m6A, including RNA stability [17,18]. Therefore, knocking down or overexpressing these m6A regulators will affect the tumor immune status.

The embryonic lethal abnormal vision (ELAV) family are RNA binding proteins, and ELAVL1 is known as human antigen R protein and is widely expressed in tissues including the small intestine, spleen, and ovaries [21]. Previous studies have confirmed that ELAVL1 is highly expressed in multiple tumors, promotes tumor occurrence and progression, and is associated with various tumor biological activities, including proliferation, migration, invasion, apoptosis, cell cycle progression, chemotherapy resistance, and radiation resistance [22,23]. ELAVL1-mediated regulation of downstream targets relies on regulating RNA stability and translation [24-26]. Recently, ELAVL1 was shown to be an m6A binding protein that relies on m6A to regulate the RNA stability and translation of downstream targets [27-29]. In tumors, ELAVL1 has been shown to regulate tumor immunity [30-32]. Moreover, ELAVL1 relies on m6A to regulate downstream targets such as CMTM6 and MIR155HG to indirectly regulate the expression of PD-L1 [32,33]. However, it has not been reported whether ELAVL1 is related to PD-L1 in PCa or the relationship between ELAVL1 and PCa.

In this study, we found that ELAVL1 was highly expressed in PCa, and high expression of ELAVL1 in PCa was associated with tumor immunosuppression. Further research showed that PD-L1 was highly expressed in PCa cells and was regulated by m6A. ELAVL1 regulated the stability of *PD-L1* mRNA in an m6A-dependent manner, which further affected the infiltration of CD4-positive T cells. Additionally, ELAVL1 expression was regulated upstream by androgen receptor (AR), but AR was also regulated by ELAVL1, and there was a mutual regulatory effect between AR and ELAVL1, which synergistically regulated the expression of PD-L1.

Materials and methods

Cell lines and experimental animals

The normal human prostate epithelial cell line RWPE-1 (GNHu37), human PCa cell line LNCaP (SCSP-5021), 22RV1 cells (SCSP-5022), PC-3 cells (TCHu158), VCaP cells (TCHu220), and the mouse PCa cell line RM-1 (TCM14) were purchased from the National Collection of Authenticated Cell Cultures (Shanghai, China). The human PCa cell line DU145 (1101HUM-PUMC000006) was purchased from the National Infrastructure of Cell Line Resource (Beijing, China). RWPE-1 cells were cultured in PEpiCM (ScienCell, # 4411), and LNCaP cells were cultured in RPMI 1640 (BasalMedia, # L210KJ) containing 10 % FBS (NEWZERUM, # FBS-S500) supplemented with 0.2 % L-glutamine (BasalMedia, # S210JV) and sodium pyruvate (BasalMedia, S410JV). 22RV1, PC-3, DU145, and RM-1 cells were cultured in RPMI 1640 (BasalMedia, # L210KJ) containing 10 % FBS (NEWZERUM, # FBS-S500), and VCaP cells were cultured in DMEM (BasalMedia, # L110KJ) containing 10 % FBS (NEWZERUM, # FBS-S500). Eight-week-old wild-type C57BL/6 mice were purchased from Vital River. All animal experiments and euthanasia were approved and performed in accordance with the guidelines of the Ethics Committee of Gongli Hospital of Shanghai Pudong New Area.

Antibodies and primers for RT–qPCR

In this study, all antibodies are listed in Table S1 in supplementary file 1. The primers for RT−qPCR are listed in Table S2 in supplementary file 1.

Immunohistochemical staining (IHC)

Tissue was fixed with 4 % paraformaldehyde (PFA) (Sigma, #158127), embedded in paraffin and sliced. Sections or PCa tissue chips (HProA150PG02) purchased from Shanghai Outdo Biotech Co., Ltd (Shanghai, China) were dewaxed with xylene and rinsed sequentially with 100 %, 95 %, and 75 % ethanol. Then, the sections were heated in citric acid at 95°C for 10 min for antigen retrieval. Subsequently, endogenous catalase was blocked by treatment with 3 % hydrogen peroxide at room temperature for 10 min. The sections were then incubated with primary antibodies, followed by horseradish peroxidase-labeled secondary antibodies. Finally, the sections were stained with diaminobenzidine and counterstained with hematoxylin.

Real-time quantitative polymerase chain reaction (RT−qPCR)

Total RNA was extracted with TRIzol reagent according to the instructions of the manufacturer (Invitrogen, #15596026) and reverse-transcribed into cDNA using ReverTra Ace qPCR RT master mix with gDNA remover (Toyobo, #fsq-301), and RT−qPCR was performed using Thunderbird SYBR qPCR mix (Toyobo, #qps-201).

Western blotting

Total protein was extracted, and an appropriate amount of denatured protein was separated by electrophoresis and electrically transferred to a membrane. After the membrane was incubated with 5 % blocking solution for 1 h, primary antibodies against each protein of interest were added and incubated with the membrane overnight at 4°C. Then, the appropriate secondary antibodies were added and incubated with the membrane at room temperature for 1 h or overnight at 4°C. Finally, the membrane was visualized with an enhanced chemiluminescence reagent (Tanon, #180-501).

RNA immunoprecipitation (RIP)-qPCR

RIP was performed as previously reported [34]. Briefly, the cells were collected and lysed with nondenaturing lysis buffer on ice for 30 min. After centrifugation, the supernatant was collected, and the protein was quantified with a bicinchoninic assay kit (Genstar, #RE162-05) according to the manufacturer's instructions. An appropriate amount of

supernatant was mixed with the primary antibody and incubated at 4°C for 6 h. Then, an appropriate amount of BSA-blocked protein A/G magnetic beads (Thermo Scientific, #26162) was added to the previous mixture, which included the primary antibody and supernatant, and incubated at 4°C overnight. After being washed twice with low-salt Tris buffer and high-salt buffer, the magnetic beads were resuspended in lysis buffer, and an appropriate amount of the sample was used for Western blotting to verify the IP efficiency. The remaining magnetic beads were collected, and the proteins were eluted with protein K buffer at 55°C for 30 min. The precipitated RNA was collected with an RNeasy MinElute® cleanup kit (Qiagen, #74204). The precipitated RNA was reverse transcribed into cDNA using ReverTra Ace qPCR RT master mix with gDNA remover (Toyobo, #fsq-301), and qPCR was performed with Thunderbird SYBR qPCR mix (Toyobo, #qps-201). Relative mRNA levels were calculated as follows: 2^ (CtIP-CtIgG), and then Student's t test was used to analyze significant differences between the groups.

Small interfering RNA (siRNA) and plasmid transfection and lentivirus infection

siRNA transfection was performed using an RFect transfection kit (Changzhou Bio-generating Biotechnology, #11012) according to the manufacturer's protocols. Plasmid transfection was performed by Lipofectamine™ 3000 reagent (Invitrogen, L3000001). In this study, all sequence of siRNA and shRNA are listed in Table S3 in supplementary file 1.

To construct the RM-1 cell line with constitutive knockdown of ELAVL1, lentiviruses expressing the empty vector (EV) and shELAVL1 were purchased from WZ Biosciences Inc. (Shandong, China). RM-1 cells were transduced with the lentiviruses and selected via the limited dilution assay.

Bioinformatic analysis of m6A-seq data

GSE147885, which includes RWPE-1 and LNCaP m6A-seq data, was obtained from the GEO database. The exomePeak R package was used to identify m6A peaks in each sample, and HOMER software was used to determine the conserved motifs within these regions. Furthermore, we divided the 3′UTR, coding sequence region (CDS), and 5′UTR regions of the longest transcript of each gene into 100 equally sized bins to characterize the distribution patterns of m6A peaks. The percentage of m6A peaks in each bin was calculated to represent the occupancy of m6A along with the transcripts. Differentially methylated regions (DMRs) were further identified using exomePeak software.

m^6A immunoprecipitation (MeRIP)-qPCR

Total RNA was extracted by using TRIzol reagent according to the instructions of the manufacturer (Invitrogen, #15596026). Total RNA (20 μg) was fragmented into 100∼200 nt fragments using RNA fragmentation agents (Thermo Fisher, #AM8740). The fragmented RNA was incubated with anti-m6A antibodies at 4°C for 4 h, and Dynabeads™ Protein A was added for immunoprecipitation (Thermo Fisher, #10002D) at 4°C for 2 h. The beads were washed five times with IPP buffer (150 mM NaCl, 0.1 % NP-40, 10 mM Tris-HCl, pH 7.4), and the immunoprecipitated RNA was recovered by elution with m6A nucleotides followed by ethanol precipitation and then reverse-transcribed into cDNA using ReverTra Ace qPCR RT master mix with gDNA remover (Toyobo, #fsq-301). qPCR was performed using Thunderbird SYBR qPCR mix (Toyobo, #qps-201).

Dual-luciferase reporter assay

Based on the m6A sequencing data from GSE147885 and our bioinformatics results, m6A-enriched regions in PD-L1 were selected. The DNA fragment corresponding to the region was ordered from Tsingke Biotechnology Co., Ltd. (Shanghai, China), and the predicted m6A sites were replaced with T. Wild-type and mutated fragments were inserted downstream of firefly luciferase in the pGL3-promoter vector.

For the dual-luciferase reporter assay, 1,900 ng of wild-type or mutant plasmids and 100 ng of pRL-TK were cotransfected into cells in a 6-well plate. After 48 h, luciferase activity was measured by using a Dual-Luciferase Reporter Assay System (Beyotime Biotechnology, #RG088S).

RNA stability assay

RNA stability assay was performed as previously reported [35]. Twenty-four hours after siRNA transfection, the cells were trypsinized and seeded into 6-well plates. After 24 h of incubation, actinomycin D (Sigma, #A9415) was added to each well at a final concentration of 5 μg/mL. After 0 h, 1 h, 2 h and 3 h, the cells were harvested and subjected to RT−qPCR to quantitatively analyze the target genes. The 18S gene was used as a negative control. The degradation rate of RNA was calculated using the following equation:

$$Nt/N0 = e - kt.$$

In vivo study

All animal experiments were conducted according to NIH guidelines and were approved by the Ethics Committees of Gongli Hospital of Shanghai Pudong New Area. Mouse prostate cancer cell line RM-1 (3×10^6) with constitutive knockdown of ELAVL1 or control cells were subcutaneously injected into the back of 4-week-old male C57BL/6 mice. The shELAVL1 group and the control group had six mice each. After two weeks, the tumors were collected and weighed.

Statistical analysis

Statistical analyses were performed using GraphPad Prism 8.0 software. The data are reported as the mean ± SD, and p values were calculated using two-tailed Student's t test; $p < 0.05$ was considered statistically significant.

Details of other bioinformatics methods are provided in the **Supplementary file 1**.

Results

ELAVL1 is highly expressed in PCa and is associated with tumor progression

Accumulating evidence has confirmed that ELAVL1 promotes the occurrence and development of tumors as an oncogene [22,23]. In the Human Protein Atlas database, high expression of ELAVL1 is present in most tumors, and in PCa and glioma, it is present in almost all patients (Fig. 1a). In the TCGA PCa database and **Human Protein Atlas** database, *ELAVL1* expression level in tumors is significantly higher than that in adjacent normal tissues (Fig. 1b-c). In the paired samples, *ELAVL1* expression in most PCa samples was higher than that in adjacent normal tissues (Fig. 1d). As the Gleason score of PCa increases, *ELAVL1* expression gradually increases (Fig. 1e), as does the T stage (Fig. 1f), suggesting that high expression of ELAVL1 in PCa is closely related to tumor progression. To verify these results, a PCa tissue chip containing 95 PCa samples was used. Total ELAVL1 expression in PCa was significantly higher than that in adjacent normal tissues (Fig. 1g-h). In addition, it has reported that compared to that in normal tissues, ELAVL1 expression in the cytoplasm of cancer cells was significantly increased, and ELAVL1 expression in the cytoplasm was related to the occurrence and progression of tumors [36]. In this study, we found that ELAVL1 expression in the cytoplasm of cancer cells was significantly higher than that in adjacent normal tissues. However, there was no difference in

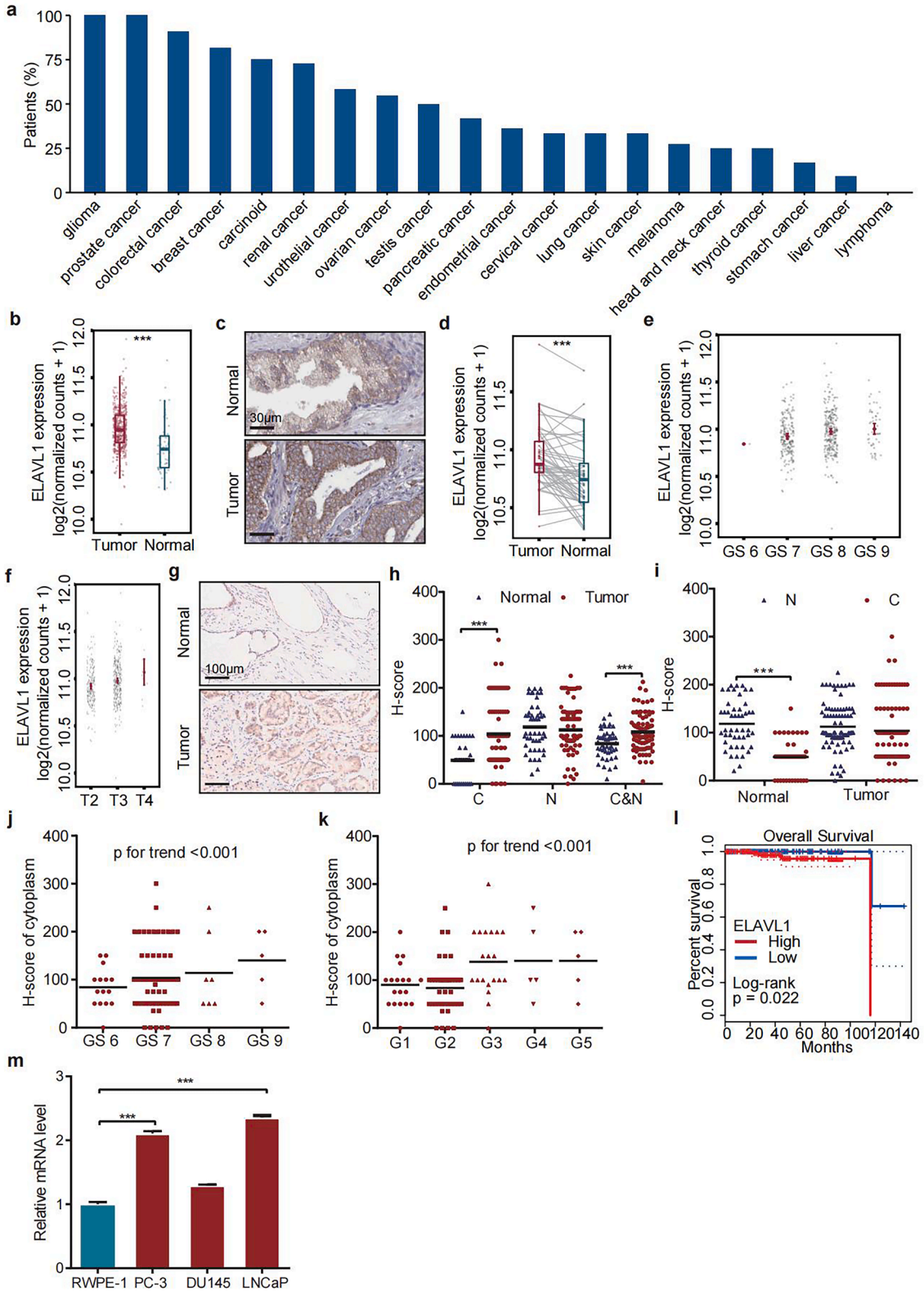

Fig. 1. ELAVL1 expression in PCa. a Rate of high ELAVL1 expression in different cancers in the **Human Protein Atlas** database. **b** ELAVL1 expression in PCa and adjacent normal prostate tissue from TCGA-PRAD data. **c** ELAVL1 expression in PCa and adjacent normal prostate tissue from the **Human Protein Atlas** database. **d** ELAVL1 expression in PCa and adjacent normal prostate tissue in paired PCa samples from TCGA-PRAD data. **e** ELAVL1 expression in samples with different Gleason scores from TCGA-PRAD data. **f** ELAVL1 expression in samples with different T stages from TCGA-PRAD data. **g** ELAVL1 expression in PCa and adjacent normal prostate tissue from the PCa tissue chip, as examined by IHC. **h-i** H-scores of ELAVL1 in the cytoplasm and nucleus of PCa and adjacent normal prostate tissue (N, nucleus; C, cytoplasm). **j** H-scores of cytoplasmic ELAVL1 in samples with different Gleason scores. **k** H-scores of cytoplasmic ELAVL1 in samples with different grades. **l** Analysis for ELAVL1 in the overall survival of PCa from the GEPIA2 database. **m** RT−qPCR showing ELAVL1 mRNA expression in different PCa cell lines. *** $p < 0.001$.

nuclear ELAVL1 expression between tumors and adjacent tissues (Fig. 1h). In adjacent normal tissues, nuclear expression of ELAVL1 was significantly higher than that in the cytoplasm. However, the expression level of ELAVL1 in the cytoplasm of tumors was similar to that in the nucleus (Fig. 1i), indicating that ELAVL1 expression in the cytoplasm is related to the occurrence and development of tumors. Further analysis showed that the expression of ELAVL1 in the cytoplasm was positively correlated with the Gleason score and grade (Fig. 1j-k). The higher the expression level of ELAVL1 in the cytoplasm, the higher the malignancy of PCa. ELAVL1 promotes tumor progression. Indeed, survival analysis confirmed that PCa patients with high ELAVL1 levels had poorer prognosis (Fig. 1l). Subsequently, we confirmed that in addition to DU145 cells, *ELAVL1* mRNA levels were higher in LNCaP and PC-3 cells than in normal prostate epithelial RWPE-1 cells (Fig. 1m). In summary, our results suggest that cytoplasmic ELAVL1 is highly expressed in PCa and is associated with tumor progression.

Given the high expression of ELAVL1 in PCa, we examined the reasons for the increase in ELAVL1 expression at the DNA level. In the TCGA-PCa dataset, we compared the copy number variations in ELAVL1 between normal tissues and PCa, and the results showed that there were more *ELAVL1* copy number variations, including the loss or amplification, in tumors than in normal tissues (Fig. 2a-b). Moreover, the loss of *ELAVL1* copy numbers led to lower expression levels than normal, while amplification increased *ELAVL1* expression (Fig. 2b). The expression of *ELAVL1* was positively correlated with copy number (Fig. 2c). We further analyzed the methylation levels of CpG sites on the *ELAVL1* gene, and the results showed that there were significant differences in methylation levels on five CpG sites between tumors and normal tissue (Fig. 2d). Among them, the methylation level on cg19590914 was positively correlated with the expression level of the *ELAVL1* gene (Fig. 2e).

ELAVL1 is associated with tumor variant characteristics in PCa

To further clarify the differences between high ELAVL1 and low ELAVL1 expression in PCa, the TCGA PCa data was divided into the high ELAVL1 and low ELAVL1 groups based on median ELAVL1 expression, and differential expression analysis was performed (Fig. 2f). GO analysis showed that the upregulated genes were mainly enriched in subsets related to RNA metabolism, while the downregulated genes were mainly enriched in tumor immunity (Fig. 2g). KEGG showed that HuR, which is also known as ELAVL1, is an important regulator of the IL17 signaling pathway, which is an important immune-related signaling pathway (Fig. S1). Then, the relationship of ELAVL1 with tumor immunity was further examined. Research has shown that microsatellite instability, copy number variation, tumor mutation burden, and tumor neoantigen load are closely related to tumor immunity and immunotherapy sensitivity [35,37-40]. In this study, focal and broad deletions of copy numbers were significantly higher in the high ELAVL1 group than in the low ELAVL1 group (Fig. 2h). The high ELAVL1 group had more total mutations and showed a positive correlation with total mutations (Fig. 2i). However, there was no difference in the number of tumor neoantigens between the high and low ELAVL1 groups (Fig. 2j). In addition, mismatch repair genes related to microsatellite instability, including MLH1, MSH2, MSH6, PMS2, and EPCAM, were significantly correlated with ELAVL1 expression (Fig. 2k). However, there was no difference in microsatellite instability scores between the high and low ELAVL1 groups (Fig. 2l). This finding indicates that the occurrence of microsatellite instability in PCa is very low.

High ELAVL1 is associated with immune suppression in PCa

To further clarify the relationship between ELAVL1 and tumor immunity, gene set enrichment analysis (GSEA) was applied to the DEGs between the high and low ELAVL1 groups. The results showed that signaling pathways related to immunity were enriched in the low ELAVL1 group (Fig. 3a). The heatmap shows that immune cells in the low ELAVL1 group were active, while immune cells in the high ELAVL1 group were suppressive (Fig. 3b). Infiltration of most types of immune cells in the high ELAVL1 group was significantly lower than that in the low ELAVL1 group (Fig. 3c). Multiple immune-related scores, including the immune score, stromal score, IMPRES, MIAS, and GEP, were significantly lower in the high ELAVL1 group than in the low ELAVL1 group, and there was a negative correlation between *ELAVL1* expression and these scores (Fig. 3d-h). Correlation analysis further showed that ELAVL1 was negatively correlated with most immune cells and the recruitment of immune cells (Fig. 3i). The CXCL family is associated with immune cell recruitment. We further analyzed the correlation between ELAVL1 and 12 molecules in the CXCL family, and the results showed that except for *CXCL9, CXCL10, CXCL11*, and *CXCL14, ELAVL1* showed a significant negative correlation with most CXCL molecules (Fig. S2), indicating that high ELAVL1 expression inhibited immune cell recruitment.

Relationship between ELAVL1 and immune regulators

In the tumor immune microenvironment, various immune regulators mediate tumor immunity. We further analyzed the correlation between the expression of ELAVL1 and various immune regulators and found that the expression levels of many immune regulators were related to *ELAVL1* expression (Fig. 4a). Among these immune regulators, five important regulators were selected, including PD-1, PD-L1, CTLA4, CD276, and LAG3. These 5 immune regulators strongly correlated with immune scores (Fig. 4b). Except for PD-1, there were significant differences in the expression levels of the other four molecules between the high and low ELAVL1 groups (Fig. 4c). Correlation analysis showed that ELAVL1 was correlated with these five regulators and had the highest correlation with *PD-L1* expression (Fig. S3a). However, only *CD276* was associated with the prognosis of PCa (Fig. 4d). Subsequently, we conducted subgroup analysis based on the expression level of ELAVL1. The results showed that in the high and low ELAVL1 groups, except for CD276, none of the other regulators had affected the prognosis within the group (Fig. S3b). Next, we further predicted the effects on the response to immune therapy based on the expression of these immune regulators, and the results showed that only ELAVL1 and PD-L1 had an impact on the effect of immune therapy (Fig. 4e). The immunotherapy response rate was lower in the high ELAVL1 group than the low ELAVL1 group, while the treatment response rate was higher in the presence of high *PD-L1* expression than low *PD-L1* expression. Unlike the other four immune regulators, PD-L1 is mainly present in tumor cells, and ELAVL1 is also expressed in tumor cells. Therefore, we selected PD-L1 as the downstream target of ELAVL1 for subsequent research.

ELAVL1 regulates PD-L1 mRNA stability in an m6A-dependent manner

Considering the high expression of ELAVL1 in hormone-sensitive PCa rather than hormone-resistant PCa (our unpublished data), we selected LNCaP and VCaP cells for subsequent experiments. We detected ELAVL1 and PD-L1 levels in different PCa cell lines, including normal prostate epithelial RWPE-1 cells and AR-positive and hormone-sensitive LNCaP and VCaP cells. Western blotting showed that ELAVL1 and PD-L1 were highly expressed in the AR-positive PCa cell lines LNCaP and VCaP (Fig. 5a). ELAVL1 is a classic RNA binding protein. Considering the correlation between ELAVL1 and PD-L1 expression in TCGA PCa data, we validated above the results in PCa tissue chip and ELAVL1 indeed positively correlated with PD-L1(Fig. S4). Next, we examined the interaction between ELAVL1 and *PD-L1* mRNA and found that ELAVL1 could bind to *PD-L1* mRNA (Fig. 5b). After knocking down ELAVL1, the mRNA and protein levels of PD-L1 were significantly reduced (Fig. 5c-d). In recent years, ELAVL1 has been shown to be an m6A binding protein that regulates RNA metabolism through m6A, including translation and stability [27-29]. Next, we found that compared to that in

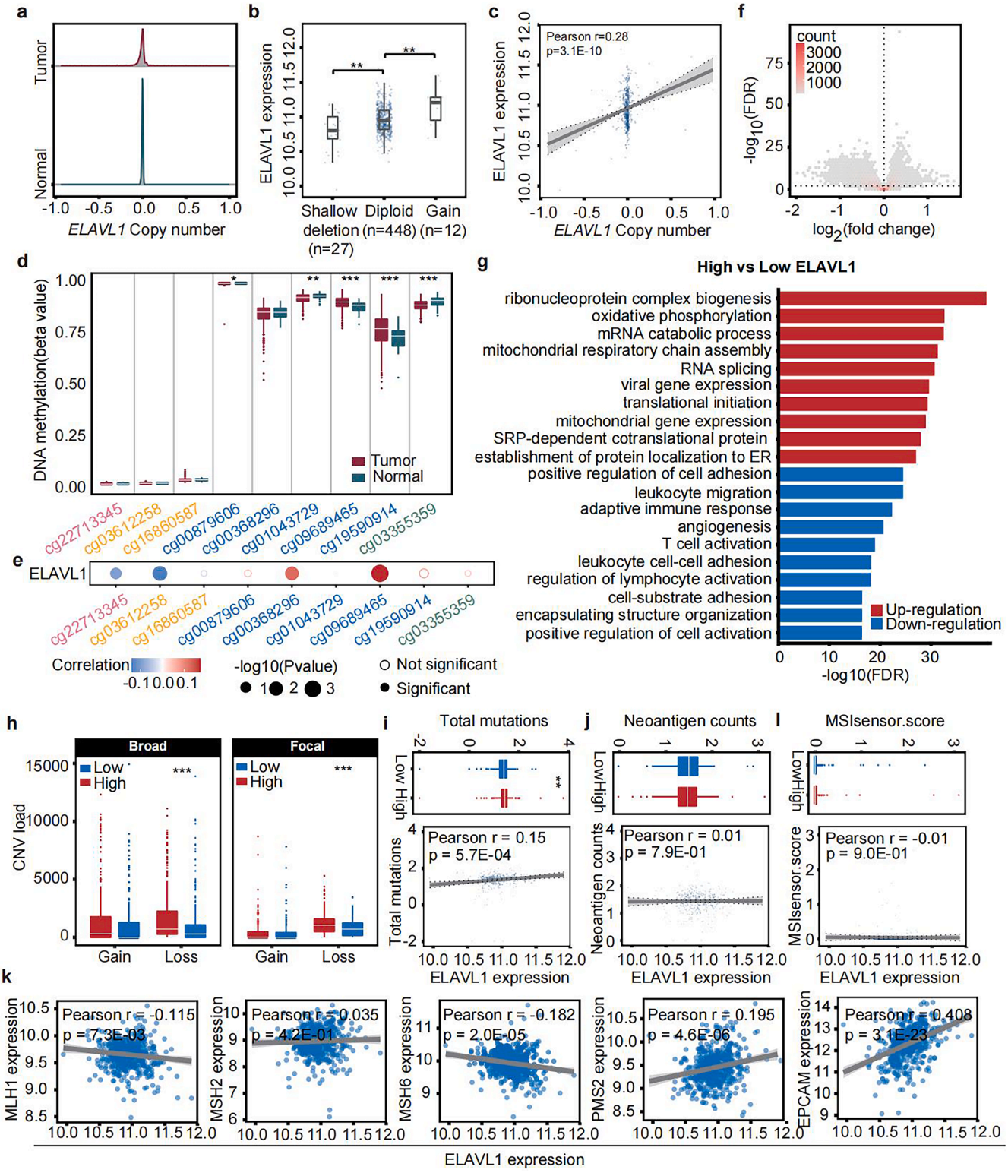

Fig. 2. ELAVL1 alterations and tumor variants at the DNA level. **a** ELAVL1 copy numbers in PCa and adjacent normal prostate tissue. **b** ELAVL1 expression in different copy number variants of ELAVL1 in PCa. **c** Correlation between ELAVL1 expression and copy number. **d** DNA methylation levels at different CpG sites of PCa and adjacent normal prostate tissue. **e** Correlation between ELAVL1 expression and methylation levels at different CpG sites of PCa. **f** Volcano plot showing differential expression analysis between the low and high ELAVL1 groups from TCGA-PARD data. **g** GO analysis of differentially expressed genes. **h** Distribution of focal and broad copy number alterations of ELAVL1 between the low and high ELAVL1 groups. **i-j** Comparison of total mutation (i) and neoantigen (j) counts between the low and high ELAVL1 groups (upper panel) and correlation between ELAVL1 expression and total mutation and neoantigen counts (lower panel). **k** Correlation between ELAVL1 expression and mismatch repair genes**. l** Comparison of MSIsensor scores between the low and high ELAVL1 groups (upper panel) and correlation between ELAVL1 expression and MSIsensor scores (lower panel). *$p<0.05$, **$p<0.01$, ***$p<0.0001$.

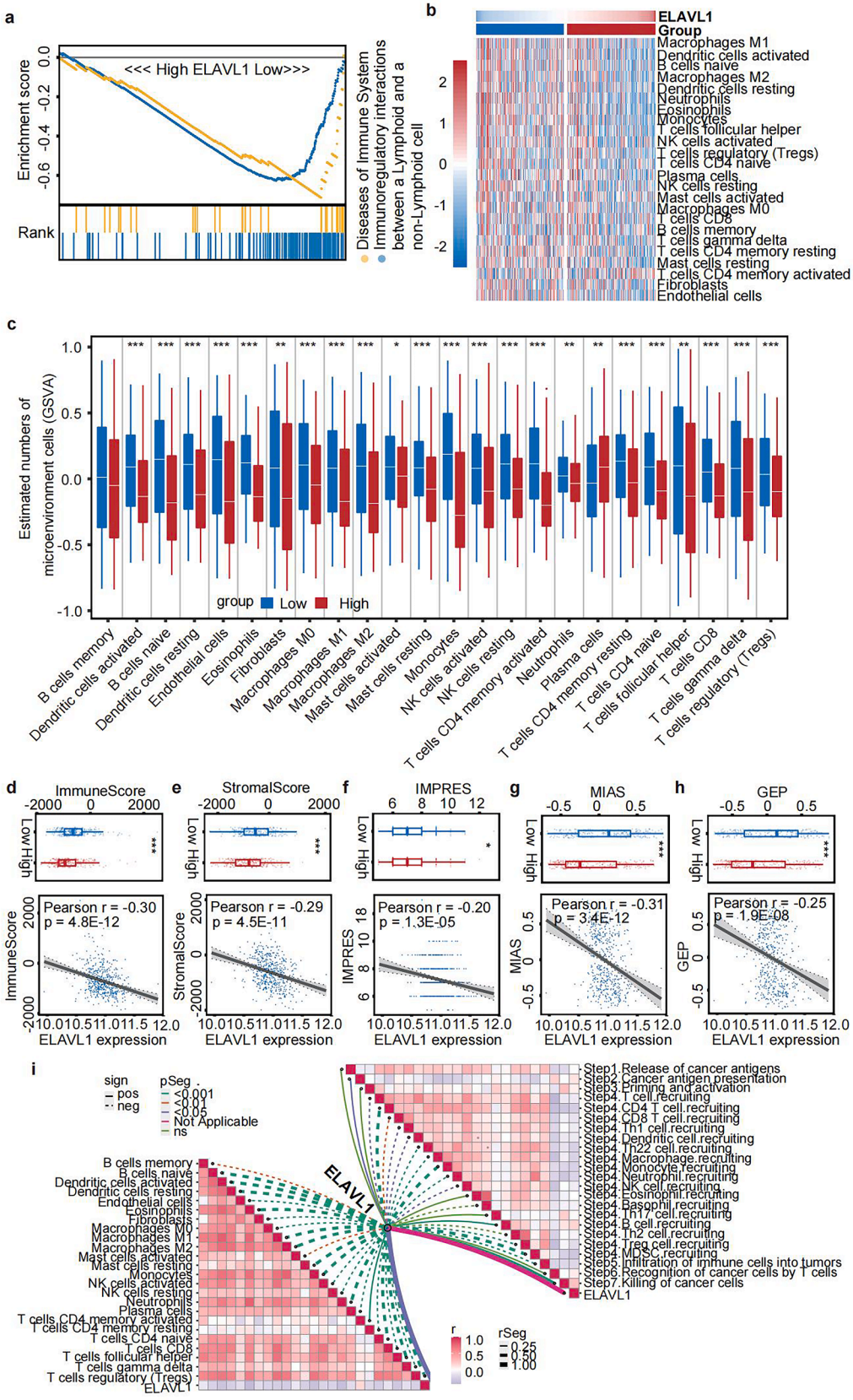

Fig. 3. Relationship between ELAVL1 and tumor immunity. a GSEA of immune-related signaling pathways between the low and high ELAVL1 groups. **b** Heatmap showing the distribution of immune cells in the low and high ELAVL1 groups. **c** Comparison of infiltrating immune cells in the low and high ELAVL1 groups. **d-h** Comparison of immune-related scores between the low and high ELAVL1 groups (upper panel) and correlation between ELAVL1 expression and immune-related scores (lower panel), including the immune score (d), stromal score (e), IMPRES (f), MIAS (g) and GEP (h). **i** Correlation between ELAVL1 expression and the steps of the cancer immunity cycle and the infiltration levels of immune cells. *$p<0.05$, **$p<0.01$, ***$p<0.0001$.

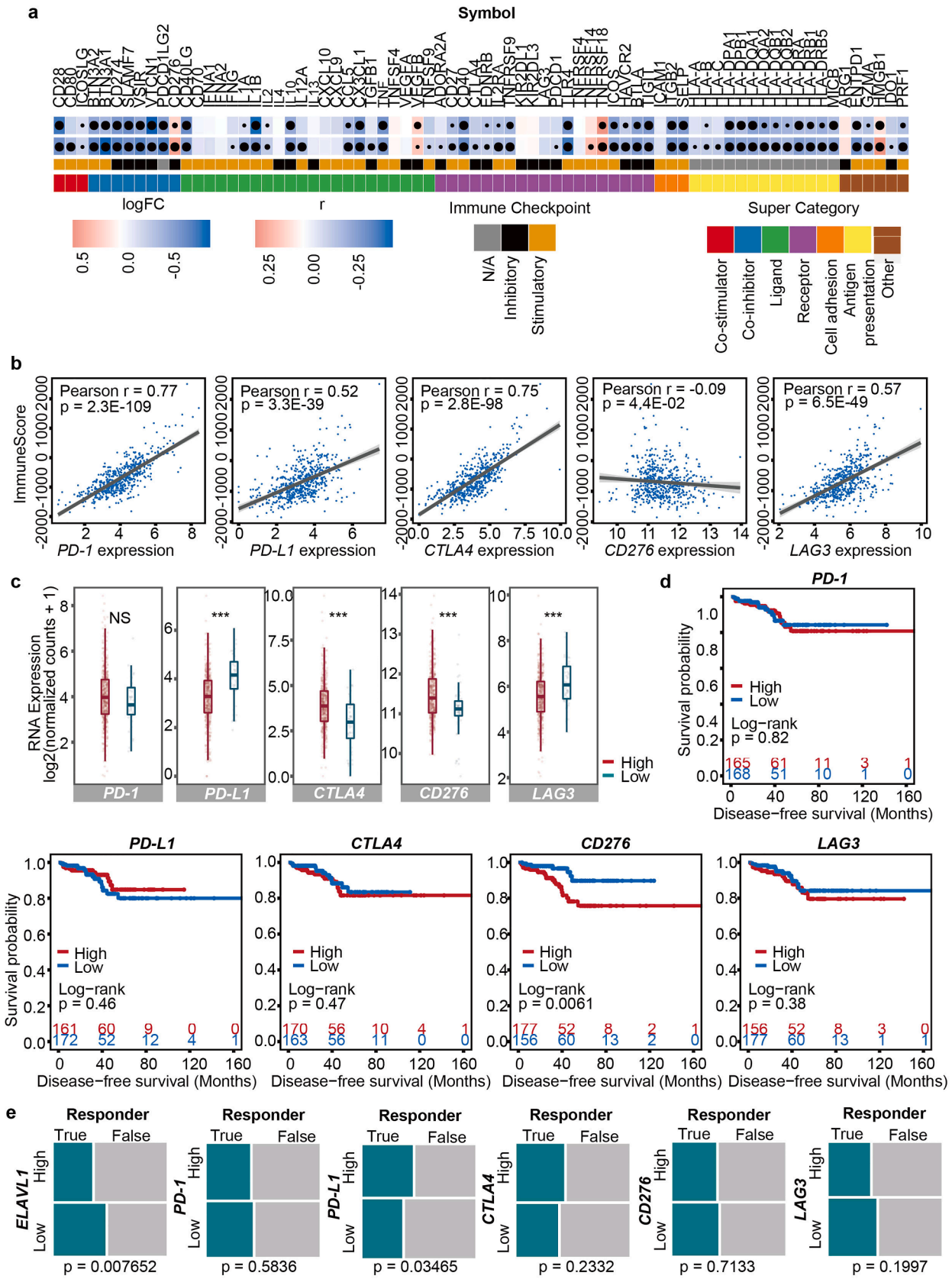

Fig. 4. ELAVL1 and immune regulators in PCa. a Correlation between ELAVL1 expression and immune regulators. **b** Correlation between the immune score and five immune regulators. **c** Comparison of five immune regulators between the low and high ELAVL1 groups. **d** Kaplan–Meier curves showing the correlation between the expression of five immune regulators and the DFI according to the TCGA database. **e** Predicted immunotherapy response rates according to ELAVL1 expression and 5 other immune regulators from the TIDE database. ***$p < 0.0001$.

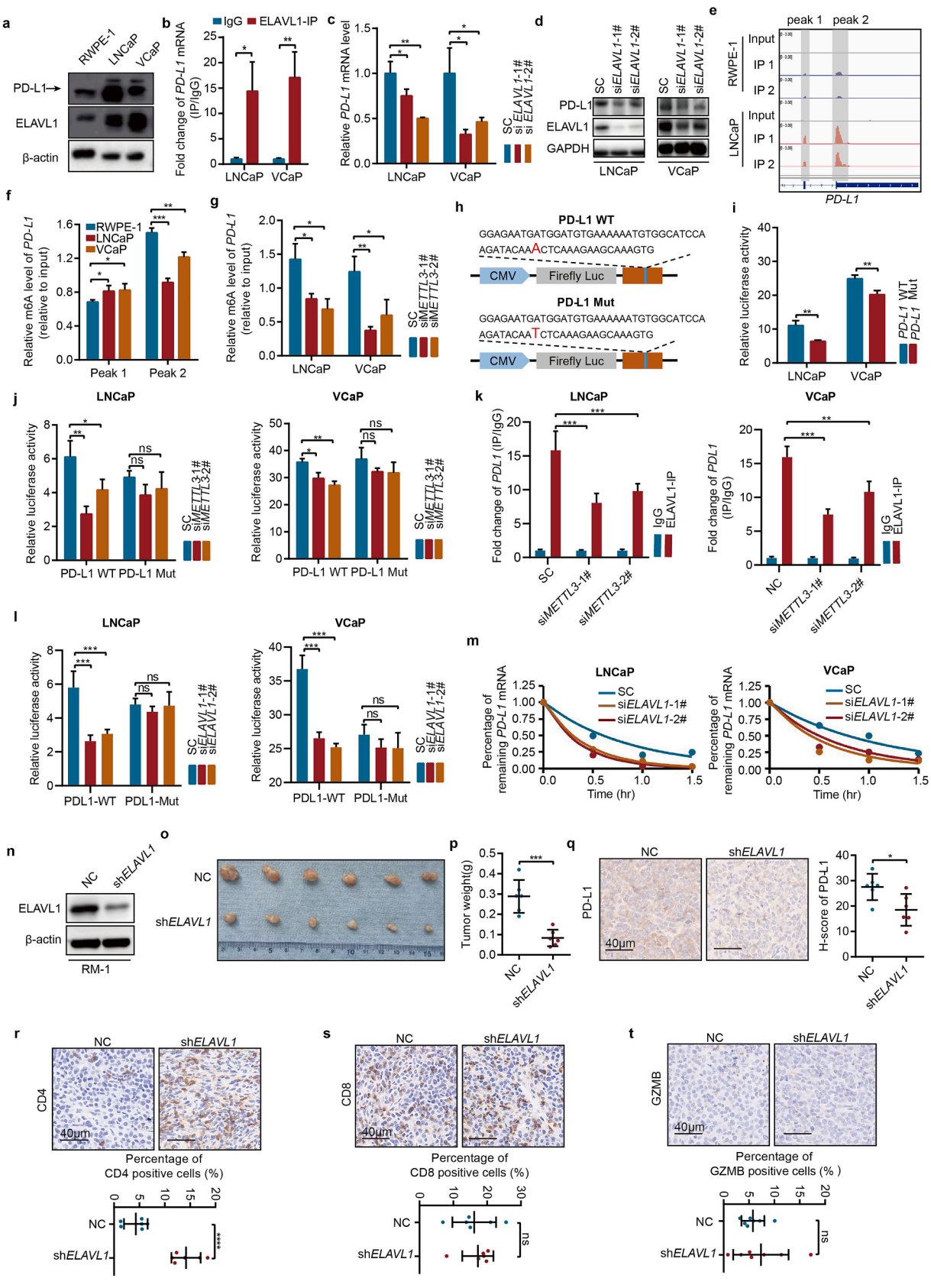

(caption on next page)

Fig. 5. ELAVL1 regulates PD-L1 via m6A. a Western blot analysis of ELAVL1 and PD-L1 in the different PCa cell lines. **b** RIP showing the interaction between ELAVL1 and PD-L1 mRNA. **c-d** PD-L1 expression was determined by RT−qPCR (c) and Western blotting (d) after ELAVL1 was silenced. **e** IgV showing PD-L1 m6A peaks. **f** MeRIP-qPCR analysis of PD-L1 m6A levels. **g** PD-L1 m6A levels were determined after silencing METTL3 by MeRIP-qPCR. **h** Diagram showing the strategy of the m6A mutation. **i** Relative luciferase activities of PD-L1 with wild-type or mutated m6A sites after being transfected into PCa cells. Firefly luciferase activity was measured and normalized to Renilla luciferase activity. **j** Relative luciferase activities of PD-L1 with wild-type or mutated m6A sites were determined after *METTL3* was silenced. **k** RIP showing the interaction change between ELAVL1 and PD-L1 mRNA after *METTL3* was silenced. **l** Relative luciferase activities of PD-L1 with wild-type or mutated m6A sites were determined after *ELAVL1* was silenced. **m** RNA stability assay to determine the effects of ELAVL1 knockdown on the half-lives (t1/2) of PD-L1. **n** Western blot analysis of ELAVL1 expression in RM-1 cells with stable silencing of ELAVL1. **o-p** Detection of the volume (o) and weight (p) of RM-1 tumors after ELAVL1 silencing. **q-t** IHC analysis of the expression of PD-L1 (q) and infiltration of CD4 (r)-, CD8 (s)- and GZMB (t)-positive cells in RM-1 tumors. $*p < 0.05$, $**p < 0.01$, $***p < 0.0001$, $****p < 0.00001$.

RWPE-1 cells, *PD-L1* had two m6A peaks in LNCaP cells, including peak 1 and peak 2 (Fig. 5e, Table S1). MeRIP-qPCR confirmed that the m6A level of peak 1 in LNCaP cells was significantly increased, while that of peak 2 was significantly reduced (Fig. 5f). Given that ELAVL1 bound to mRNA via m6A, peak 1 was selected for subsequent analysis. After knocking down *METTL3*, we found a significant decrease in the m6A level of peak 1 on PD-L1 (Fig. 5g). Subsequently, based on the m6A conserved sequence DRACH (D=A, G or U; R=A or G; H=A, C or U), we constructed a PD-L1 mutant using a point mutation of A to T on the m6A conserved sequence on Peak 1 and performed a luciferase assay (Fig. 5h). The results showed a decrease in the fluorescence activity of the PD-L1 mutant in LNCaP and VCaP cells (Fig. 5i). Moreover, knocking

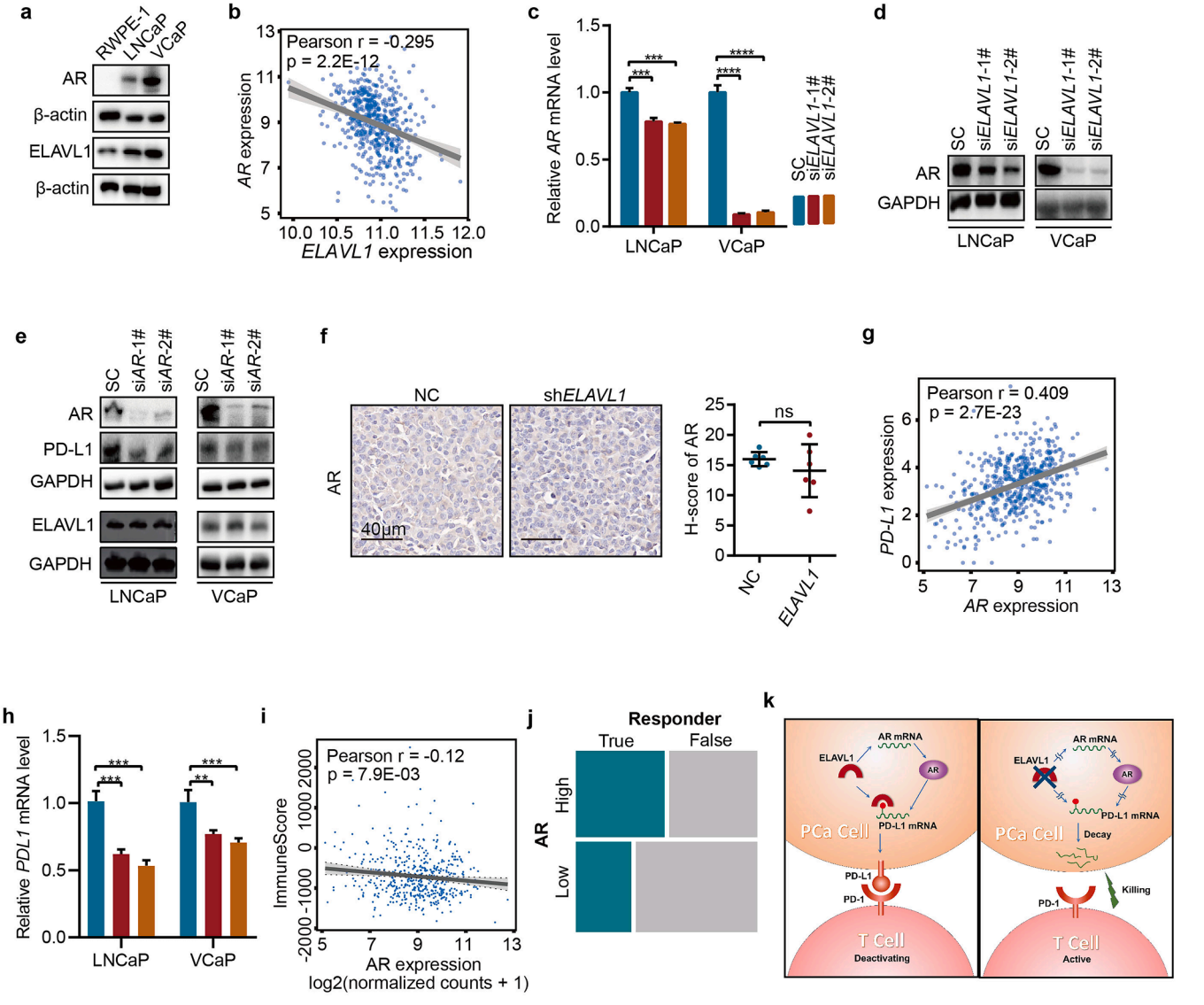

Fig. 6. ELAVL1 regulating PD-L1 expression via AR. a Western analysis of ELAVL1 and AR expression in the different PCa cell lines. **b** Correlation between ELAVL1 and AR according to the TCGA-PRAD data. **c-d** AR expression was detected by RT−qPCR (c) and Western blotting (d) after *ELAVL1* was silenced. **e** PD-L1 and ELAVL1 expression was detected by Western blotting (e) after AR was silenced. **f** IHC analysis of the expression of AR in RM-1 tumors. **g** Correlation between PD-L1 and AR according to the TCGA-PRAD data. **h** *PD-L1* expression was detected by RT−qPCR after AR was silenced. **i** Correlation between the immune score and AR according to the TCGA-PRAD data. **j** Predicted immunotherapy response rates according to AR from the TIDE database. **k** Diagram showing that the interaction between AR and ELAVL1 regulates PD-L1 mRNA stability to disrupt the infiltration of CD4-positive T cells in prostate cancer. $*p < 0.05$, $**p < 0.01$, $***p < 0.0001$, $****p < 0.00001$.

down *METTL3* in LNCaP and VCaP cells significantly reduced the luciferase activity of PD-L1-WT, while PD-L1-Mut did not (Fig. 5j). It suggested that the presence of m6A on *PD-L1* mRNA in peak 1. After knocking down *METTL3* resulting in decreased m6A in *PD-L1*, it is found that interaction between ELAVL1 and *PD-L1* mRNA wad reduced by RIP-qPCR assay (Fig. 5k). And knocking down ELAVL1 significantly reduced the luciferase activity of PD-L1-WT, while PD-L1-Mut did not (Fig. 5l). It suggested that ELAVL1 interacted with PD-L1 mRNA via m6A. Previous results showed that knocking down ELAVL1 decreased the level of *PD-L1* mRNA (Fig. 5c), which we hypothesize may be related to the regulation of mRNA stability by ELAVL1. The RNA stability assay showed that knocking down ELAVL1 significantly decreased the stability of *PD-L1* mRNA (Fig. 5m). These results indicate that ELAVL1 regulates the stability of *PD-L1* mRNA in an m6A-dependent manner.

ELAVL1 regulates PD-L1 expression in PCa cells, thereby affecting the infiltration of CD4-positive T cells

Next, we established a stable mouse prostate cancer RM-1 cell line with *ELAVL1* knockdown (Fig. 5n). Then, RM-1 with silencing *ELAVL1* was injected in the back of normal C57 mice for tumor formation. After 14 days of tumor growth, knocking down *ELAVL1* significantly reduced the volume and weight of the tumors (Fig. 5o-p). Immunohistochemistry confirmed that knocking down *ELAVL1* significantly reduced the expression of PD-L1 in the tumors (Fig. 5q). PD-L1 is associated with T-cell inhibition. In this study, knocking down *ELAVL1* significantly increased the number of CD4-positive T cells (Fig. 5r), while the number of CD8-positive T cells, cytotoxic T cells, or natural killer cells was not significantly changed, although there was an increase (Fig. 5s-t). These results indicate that ELAVL1 inhibits the infiltration of CD4-positive T cells by promoting the expression of PD-L1.

ELAVL1 inhibits tumor immunity via AR

As shown in Fig. 5a and e, ELAVL1 regulates PD-L1, which is highly expressed in AR-positive PCa cells. We hypothesize that the expression of ELAVL1 is influenced by AR. Western blotting showed a significant increase in ELAVL1 expression in LNCaP and VCaP cells compared to RWPE-1 cells, similar to AR. The higher the AR expression, the higher the ELAVL1 expression (Fig. 6a). The expression of AR and ELAVL1 may be positively correlated in hormone-sensitive PCa. However, in the TCGA-PCa dataset, there was a negative correlation between *ELAVL1* and *AR* (Fig. 6b), which may be related to the high expression of ELAVL1 in the tumor microenvironment. Subsequently, we further explored the regulatory relationship between ELAVL1 and AR. After knocking down *ELAVL1*, we found a significant decrease in the mRNA and protein expression of AR (Fig. 6c-d). However, after knocking down *AR*, ELAVL1 remains no change in LNCaP and VCaP cells (Fig. 6e). In RM-1 tumors, there was a decrease trend in AR expression after *ELAVL1* knockdown, although there was no significant difference (Fig. 6f). Above results indicated that AR is an downstream target of ELAVL1. Next, we asked whether AR also regulates *PD-L1* mRNA. Correlation analysis showed a positive correlation between *AR* and *PD-L1* (Fig. 6g), and it showed a significant decrease in *PD-L1* mRNA and protein expression after knocking down *AR* (Fig. 6e, h). We also furtherly examined the relationship between AR and tumor immunity in PCa. Gene set variation analysis (GSVA) showed that high expression of AR increased the infiltration of activated dendritic cells, eosinophils, neutrophils, and reserved memory CD4 cells and decreased the infiltration of fibroblasts, M2 macrophages, plasma cells, and regulatory T cells (Fig. S5). Correlation analysis showed a negative correlation between *AR* expression and the immune score (Fig. 6i). Finally, in PCa patients with high *AR* expression, the predicted immunotherapeutic effect as significantly higher than that in patients with low *AR* expression (Fig. 6j), which as attributed to the fact that high expression of AR led to high expression of PD-L1, thereby exerting an effect on PD-L1 inhibitors.

Discussion

ELAVL1 is a classic RNA binding protein that has been shown to be dysregulated in multiple tumors [22,23]. Accumulating evidence has shown that ELAVL1 is involved in multiple aspects of tumor biology, including proliferation, cell cycle progression, invasion, migration, and apoptosis [22,23]. In addition, ELAVL1 has also been shown to be associated with chemotherapy resistance and radiotherapy resistance [41-43]. In PCa, it has shown that ELAVL1 is highly expressed and associated with tumor development through COX2 [44]. In this study, we further confirmed that ELAVL1 was increased in PCa and that ELAVL1 was positively associated with tumor grade, Gleason score, and T stage. Tumor immunity in the tumor microenvironment is a new direction for treating tumors. It has also been reported that ELAVL1 is crucial for the development and differentiation of T and B cells [30]. The relationship between ELAVL1 and immune function in the tumor microenvironment needs to be explored. PCa is a type of tumor that responds poorly to immunotherapy [6-8]. In this study, we found a close relationship between high expression of *ELAVL1* and immune suppression in PCa. ELAVL1 is involved in the expression and regulation of many immune regulators in PCa, which may be an important molecular mechanism by which ELAVL1 regulates tumor immunity. Among these immune regulators, CTLA4, CD276, and LAG3 have been confirmed to have a close relationship with PCa immunity and are new targets for future PCa immunotherapy [45-47]. Therefore, ELAVL1 may be a promising target, and inhibiting ELAVL1 expression has the potential to enhance the immune activity of PCa.

The m6A modification is the most abundant chemical modification of mRNA in mammals [48]. It is known that an imbalance in m6A and m6A regulator expression is an important factor leading to the occurrence and development of multiple tumors and is involved in regulating the biological aspects of multiple tumors, similar to ELAVL1 [49]. In addition, m6A is involved in the functional regulation of tumor immunity [50]. The methyltransferase METTL3 can remodel the tumor microenvironment to improve the tumor immunotherapy response [51]. METTL3 also plays a role in inducing anti-PD-1 immunotherapy responses in thyroid cancer [52]. METTL16 mediates immune invasion in colorectal cancer [19]. The m6A binding protein YTHDF1 inhibits CD8 positive T-cell-mediated antitumor immunity in PCa [20]. These studies indicate that changes in RNA m6A occur in tumor immune regulators, thereby regulating tumor immunity. In PCa, there is a lack of understanding of m6A levels in immune regulators. In our study, we found the presence of m6A sites on some immune regulators and significant imbalances in m6A levels. Changes in m6A levels on these immune regulators indicate a close relationship between the immune level of PCa and m6A. Targeting m6A will be an important strategy for improving the immune response of PCa.

PD-L1 is a widely recognized immune checkpoint protein that is highly expressed in many tumors [53]. Blocking the PD-1/PD-L1 signaling pathway has shown good therapeutic efficacy in many tumors [54]. However, the immunotherapeutic response of some tumors, including PCa, is not ideal [6-8]. Therefore, understanding the regulatory mechanism of PD-L1 expression will further improve the immunotherapeutic response of these tumors. Previous studies have reported that the expression of PD-L1 is regulated at the genomic, transcriptional, posttranscriptional, and posttranslational levels [55]. In recent years, m6A, which is a posttranscriptional modification, has been shown to participate in the expression and regulation of PD-L1 in tumors, including bladder cancer, cholangiocarcinoma, hepatocellular carcinoma, and cervical cancer [17-19]. However, it has not been reported whether PD-L1 is regulated by m6A in PCa. In this study, we reported for the first time that *PD-L1* was modified by m6A in PCa. Previous studies have confirmed that m6A occurs near the stop codon of PD-L1 [17-19]. However, in this study, m6A modification of *PD-L1* occurred in the CDS region in PCa. It was found that ELAVL1, which is an m6A binding protein, relies on m6A to regulate the mRNA stability of *PD-L1*. The

regulation of *PD-L1* mRNA stability by ELAVL1 through m6A may be an important regulatory mechanism of ELAVL1-mediated immunosuppression in PCa. However, we did not examine whether there are other m6A readers that regulate the stability of PDL1 in an m6A-dependent manner. In previous studies, some m6A readers such as IGF2BP2, YTHDF3, and YTHDF1 have been found to be involved in the stability of PDL1 mRNA in tumors, thereby interfering with tumor immunity [56-58]. In prostate cancer, it has also reported that YTHDF1 inhibits the anti-tumor immunity of CD8 positive T cells through PDL1 via m6A[59]. In theory, there is competitive regulation among different m6A readers that regulate PD-L1 stability. However, there have been previous reports that ELAVL1 exerted a synergistic regulatory effect on mRNA by binding to other m6A readers such as YTHDC1 and IGF2BP1[27,60]. In prostate cancer, whether ELAVL1 competitively regulates the stability of PD-L1 with other m6A readers or synergistically regulates it requires further assays.

AR is an important transcription factor that drives the development of PCa [61]. It has found that AR is related to tumor immunity [62]. In PCa, activation of the AR signaling pathway is also found in tumor-associated macrophages [63]. Antagonizing AR can reverse the immunosuppressive state of PCa [64]. In bladder cancer, AR was shown to promote tumor immune escape by inhibiting the expression of PD-L1 [65]. Whether AR regulates tumor immunity through PD-L1 in PCa has not yet been reported. In this study, we confirmed that AR could positively regulate the expression of PD-L1 and was also regulated by ELAVL1.Therefore, the regulation of PD-L1 by AR in PCa may occur through ELAVL1, while there was a direct regulatory relationship between ELAVL1 and PD-L1.

In this study, we found that ELAVL1 was highly expressed and associated with immune suppression in PCa. ELAVL1 regulates the RNA stability of *PD-L1* through m6A, thereby regulating the infiltration of CD4-positive T cells, ultimately leading to immunosuppression in PCa. Further research also showed that AR positively regulated the expression of PD-L1, which was related to tumor immunosuppression and also was regulated by ELAVL1. This study confirms the important role of ELAVL1 in maintaining immune suppression in PCa. Targeted inhibition of ELAVL1 is expected to provide hope for reversing immune suppression in PCa and improving the response to immune therapy.

Conclusions

In this study, we have found that high expressed ELAVL1 in PCa was related to tumor immunosuprression by regulating PD-L1 mRNA stability to inhibit CD4-positive T cells infilration and PD-L1 expression also was regulated by ELAVL1 via AR.

Abbreviation

AR	Androgen receptor
CDS	Coding sequence region
CRPC	Castration-resistant prostate cancer
DMR	Differentially methylated region
ELAV	Embryonic lethal abnormal vision
EV	Empty vector
GSEA	Gene set enrichment analysis
GSVA	Gene set variation analysis
IHC	Immunohistochemical staining
MeRIP	m6A immunoprecipitation
PCa	Prostate cancer
RT−qPCR	Real-time quantitative polymerase chain reaction
RIP	RNA immunoprecipitation
siRNA	Small interfering RNA

Ethics declarations

The studies of Human prostate cancer tissue chips (HProA150PG02) in this study purchased from Shanghai Outdo Biotech Co., Ltd (Shanghai, China) were reviewed and approved by the Ethics Committee of Shanghai Outdo Biotech Company.Written informed consent was obtained from all participants for their participation in this study. The animal experiments were approved by Animal Care and Use Committee of Shanghai Ninth People's Hospital.

Funding

This work is supported by the grant from Clinical Summit Discipline Construction Project of Pudong New Area Health Commission (PYWgf2021-06), Cultivation Fund of National Natural Science Foundation of China (2023GPY-B01) and Demonstration Pilot Project of Traditional Chinese Medicine Inheritance and Innovation Development in Pudong New Area: The Construction plan of the Flagship Department of Chinese and Western Medicine Collaboration (Urology) in Pudong New Area (YC-2023-0405).

Consent for publication

All authors read and approved the final manuscript for publication.

Fund

This work is supported by the grant from Clinical Summit Discipline Construction Project of Pudong New Area Health Commission (PYWgf2021-06), Cultivation Fund of National Natural Science Foundation of China (2023GPY-B01) and Demonstration Pilot Project of Traditional Chinese Medicine Inheritance and Innovation Development in Pudong New Area: The Construction plan of the Flagship Department of Chinese and Western Medicine Collaboration (Urology) in Pudong New Area (YC-2023-0405).

CRediT authorship contribution statement

Zhonglin Cai: Writing – review & editing, Writing – original draft, Visualization, Methodology. **Xiuxia Zhai:** Writing – original draft, Methodology, Formal analysis. **Jidong Xu:** Resources, Methodology, Investigation, Formal analysis. **Tianyu Hong:** Data curation, Formal analysis, Writing – review & editing. **Kuo Yang:** Formal analysis, Methodology. **Shasha Min:** Investigation, Methodology. **Jianuo Du:** Conceptualization, Data curation, Formal analysis. **Zhikang Cai:** Supervision, Validation, Visualization. **Zhong Wang:** Visualization, Validation, Data curation, Conceptualization. **Ming Shen:** Validation, Supervision, Project administration, Methodology. **Di Wang:** Resources, Project administration, Methodology, Investigation. **Yanting Shen:** Project administration, Conceptualization.

Declaration of competing interest

The authors declare that they have no known competing financial interests or personal relationships that could have appeared to influence the work reported in this paper.

Data availability

All data needed to evaluate the conclusions in the paper are present in the paper or the Supplementary Materials. Materials described in the study are available on request from the corresponding author.

Acknowledgements

Not applicable

Supplementary materials

Supplementary material associated with this article can be found, in the online version, at doi:10.1016/j.neo.2024.101049.

References

[1] H Sung, J Ferlay, RL Siegel, M Laversanne, I Soerjomataram, A Jemal, F Bray, Global cancer statistics 2020: GLOBOCAN estimates of incidence and mortality worldwide for 36 cancers in 185 Countries, CA Cancer J. Clin. 71 (3) (2021) 209–249.

[2] RL Siegel, KD Miller, HE Fuchs, A Jemal, Cancer Statistics, 2021, CA Cancer J. Clin. 71 (1) (2021) 7–33.

[3] M Cai, XL Song, XA Li, M Chen, J Guo, DH Yang, Z Chen, SC Zhao, Current therapy and drug resistance in metastatic castration-resistant prostate cancer, Drug Resist. Updat. 68 (2023) 100962.

[4] JS de Bono, C Guo, B Gurel, AM De Marzo, KS Sfanos, RS Mani, J Gil, CG Drake, A Alimonti, Prostate carcinogenesis: inflammatory storms, Nat. Rev. Cancer 20 (8) (2020) 455–469.

[5] TE Krueger, DLJ Thorek, AK Meeker, JT Isaacs, WN Brennen, Tumor-infiltrating mesenchymal stem cells: drivers of the immunosuppressive tumor microenvironment in prostate cancer? Prostate 79 (3) (2019) 320–330.

[6] DP Petrylak, Y Loriot, DR Shaffer, F Braiteh, J Powderly, LC Harshman, P Conkling, JP Delord, M Gordon, JW Kim, et al., Safety and clinical activity of atezolizumab in patients with metastatic castration-resistant prostate cancer: a phase I study, Clin. Cancer Res. 27 (12) (2021) 3360–3369.

[7] AR Hansen, C Massard, PA Ott, NB Haas, JS Lopez, S Ejadi, JM Wallmark, B Keam, JP Delord, R Aggarwal, et al., Pembrolizumab for advanced prostate adenocarcinoma: findings of the KEYNOTE-028 study, Ann. Oncol. 29 (8) (2018) 1807–1813.

[8] K Fizazi, CG Drake, TM Beer, ED Kwon, HI Scher, WR Gerritsen, A Bossi, A den Eertwegh, M Krainer, N Houede, et al., Final analysis of the ipilimumab versus placebo following radiotherapy phase III trial in postdocetaxel metastatic castration-resistant prostate cancer identifies an excess of long-term survivors, Eur. Urol. 78 (6) (2020) 822–830.

[9] D Nava Rodrigues, P Rescigno, D Liu, W Yuan, S Carreira, MB Lambros, G Seed, J Mateo, R Riisnaes, S Mullane, et al., Immunogenomic analyses associate immunological alterations with mismatch repair defects in prostate cancer, J. Clin. Invest. 128 (10) (2018) 4441–4453.

[10] HB Kaur, LB Guedes, J Lu, L Maldonado, L Reitz, JR Barber, AM De Marzo, JJ Tosoian, SA Tomlins, EM Schaeffer, et al., Association of tumor-infiltrating T-cell density with molecular subtype, racial ancestry and clinical outcomes in prostate cancer, Mod. Pathol. 31 (10) (2018) 1539–1552.

[11] N Vitkin, S Nersesian, DR Siemens, M Koti, The tumor immune contexture of prostate cancer, Front. Immunol. 10 (2019) 603.

[12] T Vidotto, FP Saggioro, T Jamaspishvili, DL Chesca, CG Picanco de Albuquerque, RB Reis, CH Graham, DM Berman, DR Siemens, JA Squire, et al., PTEN-deficient prostate cancer is associated with an immunosuppressive tumor microenvironment mediated by increased expression of IDO1 and infiltrating FoxP3+ T regulatory cells, Prostate 79 (9) (2019) 969–979.

[13] P Xu, LJ Wasielewski, JC Yang, D Cai, CP Evans, WJ Murphy, C Liu, The immunotherapy and immunosuppressive signaling in therapy-resistant prostate cancer, Biomedicines. 10 (8) (2022).

[14] JD Wolchok, V Chiarion-Sileni, R Gonzalez, P Rutkowski, JJ Grob, CL Cowey, CD Lao, J Wagstaff, D Schadendorf, PF Ferrucci, et al., Overall survival with combined nivolumab and ipilimumab in advanced melanoma, N. Engl. J. Med. 377 (14) (2017) 1345–1356.

[15] RJ Motzer, NM Tannir, DF McDermott, O Aren Frontera, B Melichar, TK Choueiri, ER Plimack, P Barthelemy, C Porta, S George, et al., Nivolumab plus Ipilimumab versus Sunitinib in Advanced Renal-Cell Carcinoma, N. Engl. J. Med. 378 (14) (2018) 1277–1290.

[16] Y Zhao, Y Ma, Y Fan, J Zhou, N Yang, Q Yu, W Zhuang, W Song, ZM Wang, B Li, et al., A multicenter, open-label phase Ib/II study of cadonilimab (anti PD-1 and CTLA-4 bispecific antibody) monotherapy in previously treated advanced non-small-cell lung cancer (AK104-202 study), Lung Cancer 184 (2023) 107355.

[17] Z Ni, P Sun, J Zheng, M Wu, C Yang, M Cheng, M Yin, C Cui, G Wang, L Yuan, et al., JNK signaling promotes bladder cancer immune escape by regulating METTL3-mediated m6A modification of PD-L1 mRNA, Cancer Res. 82 (9) (2022) 1789–1802.

[18] X Qiu, S Yang, S Wang, J Wu, B Zheng, K Wang, S Shen, S Jeong, Z Li, Y Zhu, et al., M(6)A demethylase ALKBH5 regulates PD-L1 expression and tumor immunoenvironment in intrahepatic cholangiocarcinoma, Cancer Res. 81 (18) (2021) 4778–4793.

[19] A Wang, Y Sun, X Wang, Z Yan, D Wang, L Zeng, Q Lu, m(6)A methyltransferase METTL16 mediates immune evasion of colorectal cancer cells via epigenetically regulating PD-L1 expression, Aging (Albany. NY) 15 (16) (2023) 8444–8457.

[20] Y Wang, P Jin, X Wang, N(6)-methyladenosine regulator YTHDF1 represses the CD8 + T cell-mediated antitumor immunity and ferroptosis in prostate cancer via m(6)A/PD-L1 manner, Apoptosis. (2023).

[21] S Srikantan, M Gorospe, HuR function in disease, Front. Biosci. (Landmark. Ed) 17 (1) (2012) 189–205.

[22] D Goutas, A Pergaris, C Giaginis, S Theocharis, HuR as therapeutic target in cancer: what the future holds, Curr. Med. Chem. 29 (1) (2022) 56–65.

[23] X Wu, L Xu, The RNA-binding protein HuR in human cancer: A friend or foe? Adv. Drug Deliv. Rev. 184 (2022) 114179.

[24] CM Brennan, JA Steitz, HuR and mRNA stability, Cell Mol. Life Sci. 58 (2) (2001) 266–277.

[25] I Grammatikakis, K Abdelmohsen, M Gorospe, Posttranslational control of HuR function, Wiley. Interdiscip. Rev. RNa 8 (1) (2017).

[26] MR Smith, G Costa, RNA-binding proteins and translation control in angiogenesis, FEBS. J. 289 (24) (2022) 7788–7809.

[27] D Liang, WJ Lin, M Ren, J Qiu, C Yang, X Wang, N Li, T Zeng, K Sun, L You, et al., m(6)A reader YTHDC1 modulates autophagy by targeting SQSTM1 in diabetic skin, Autophagy. 18 (6) (2022) 1318–1337.

[28] Y Chen, C Peng, J Chen, D Chen, B Yang, B He, W Hu, Y Zhang, H Liu, L Dai, et al., WTAP facilitates progression of hepatocellular carcinoma via m6A-HuR-dependent epigenetic silencing of ETS1, Mol. Cancer 18 (1) (2019) 127.

[29] B Yue, C Song, L Yang, R Cui, X Cheng, Z Zhang, G Zhao, METTL3-mediated N6-methyladenosine modification is critical for epithelial-mesenchymal transition and metastasis of gastric cancer, Mol. Cancer 18 (1) (2019) 142.

[30] M Majumder, P Chakraborty, S Mohan, S Mehrotra, V Palanisamy, HuR as a molecular target for cancer therapeutics and immune-related disorders, Adv. Drug Deliv. Rev. 188 (2022) 114442.

[31] Y Huang, L Xia, X Tan, J Zhang, W Zeng, B Tan, X Yu, W Fang, Z Yang, Molecular mechanism of lncRNA SNHG12 in immune escape of non-small cell lung cancer through the HuR/PD-L1/USP8 axis, Cell Mol. Biol. Lett. 27 (1) (2022) 43.

[32] J Li, X Dong, X Kong, Y Wang, Y Li, Y Tong, W Zhao, W Duan, P Li, Y Wang, et al., Circular RNA hsa_circ_0067842 facilitates tumor metastasis and immune escape in breast cancer through HuR/CMTM6/PD-L1 axis, Biol. Direct. 18 (1) (2023) 48.

[33] L Peng, B Pan, X Zhang, Z Wang, J Qiu, X Wang, N Tang, Lipopolysaccharide facilitates immune escape of hepatocellular carcinoma cells via m6A modification of lncRNA MIR155HG to upregulate PD-L1 expression, Cell Biol. Toxicol. 38 (6) (2022) 1159–1173.

[34] R Huang, L Yang, Z Zhang, X Liu, Y Fei, WM Tong, Y Niu, Z Liang, RNA m(6)A demethylase ALKBH5 protects against pancreatic ductal adenocarcinoma via targeting regulators of iron metabolism, Front. Cell Dev. Biol. 9 (2021) 724282.

[35] ZW Zhang, X Teng, F Zhao, C Ma, J Zhang, LF Xiao, Y Wang, M Chang, Y Tian, C Li, et al., METTL3 regulates m(6)A methylation of PTCH1 and GLI2 in Sonic hedgehog signaling to promote tumor progression in SHH-medulloblastoma, Cell Rep. 41 (4) (2022) 111530.

[36] N Melling, B Taskin, C Hube-Magg, M Kluth, S Minner, C Koop, T Grob, M Graefen, H Heinzer, MC Tsourlakis, et al., Cytoplasmic accumulation of ELAVL1 is an independent predictor of biochemical recurrence associated with genomic instability in prostate cancer, Prostate 76 (3) (2016) 259–272.

[37] R Cohen, B Rousseau, J Vidal, R Colle, LA Diaz Jr., T Andre, Immune checkpoint inhibition in colorectal cancer: microsatellite instability and beyond, Target. Oncol. 15 (1) (2020) 11–24.

[38] S Das, DB Johnson, Immune-related adverse events and anti-tumor efficacy of immune checkpoint inhibitors, J. ImmunOther Cancer 7 (1) (2019) 306.

[39] TE Keenan, KP Burke, EM Van Allen, Genomic correlates of response to immune checkpoint blockade, Nat. Med. 25 (3) (2019) 389–402.

[40] DL Jardim, A Goodman, D de Melo Gagliato, R Kurzrock, The challenges of tumor mutational burden as an immunotherapy biomarker, Cancer Cell 39 (2) (2021) 154–173.

[41] Q Ma, Q Lu, X Lei, J Zhao, W Sun, D Huang, Q Zhu, Q Xu, Relationship between HuR and tumor drug resistance, Clin. Transl. Oncol. 25 (7) (2023) 1999–2014.

[42] Z Ju, M Lei, L Xuan, J Luo, M Zhou, Y Wang, L Shen, M Skonieczna, DS Ivanov, HMH Zakaly, et al., P53-response circRNA_0006420 aggravates lung cancer radiotherapy resistance by promoting formation of HUR/PTBP1 complex, J. Adv. Res. (2023).

[43] M Mehta, K Basalingappa, JN Griffith, D Andrade, A Babu, N Amreddy, R Muralidharan, M Gorospe, T Herman, WQ Ding, et al., HuR silencing elicits oxidative stress and DNA damage and sensitizes human triple-negative breast cancer cells to radiotherapy, Oncotarget. 7 (40) (2016) 64820–64835.

[44] F Barbisan, R Mazzucchelli, A Santinelli, A Lopez-Beltran, L Cheng, M Scarpelli, F Montorsi, R Montironi, Overexpression of ELAV-like protein HuR is associated with increased COX-2 expression in atrophy, high-grade prostatic intraepithelial neoplasia, and incidental prostate cancer in cystoprostatectomies, Eur. Urol. 56 (1) (2009) 105–112.

[45] CD Zahm, JE Moseman, LE Delmastro, GM D, PD-1 and LAG-3 blockade improve anti-tumor vaccine efficacy, Oncoimmunology. 10 (1) (2021) 1912892.

[46] W Shi, Y Wang, Y Zhao, JJ Kim, H Li, C Meng, F Chen, J Zhang, DH Mak, V Van, et al., Immune checkpoint B7-H3 is a therapeutic vulnerability in prostate cancer harboring PTEN and TP53 deficiencies, Sci. Transl. Med. 15 (695) (2023) eadf6724.

[47] SK Subudhi, BA Siddiqui, AM Aparicio, SS Yadav, S Basu, H Chen, S Jindal, RSS Tidwell, A Varma, CJ Logothetis, et al., Combined CTLA-4 and PD-L1 blockade in patients with chemotherapy-naive metastatic castration-resistant prostate cancer is associated with increased myeloid and neutrophil immune subsets in the bone microenvironment, J. ImmunOther Cancer 9 (10) (2021).

[48] X Jiang, B Liu, Z Nie, L Duan, Q Xiong, Z Jin, C Yang, Y Chen, The role of m6A modification in the biological functions and diseases, Signal. Transduct. Target. Ther. 6 (1) (2021) 74.

[49] Q Lan, PY Liu, J Haase, JL Bell, S Huttelmaier, T Liu, The Critical Role of RNA m(6) a methylation in cancer, Cancer Res. 79 (7) (2019) 1285–1292.

[50] L Chen, Y He, J Zhu, S Zhao, S Qi, X Chen, H Zhang, Z Ni, Y Zhou, G Chen, et al., The roles and mechanism of m(6)A RNA methylation regulators in cancer immunity, Biomed. PharmacOther 163 (2023) 114839.

[51] H Yu, J Liu, X Bu, Z Ma, Y Yao, J Li, T Zhang, W Song, X Xiao, Y Sun, et al., Targeting METTL3 reprograms the tumor microenvironment to improve cancer immunotherapy, Cell Chem. Biol. (2023).
[52] J Ning, X Hou, J Hao, W Zhang, Y Shi, Y Huang, X Ruan, X Zheng, M Gao, METTL3 inhibition induced by M2 macrophage-derived extracellular vesicles drives anti-PD-1 therapy resistance via M6A-CD70-mediated immune suppression in thyroid cancer, Cell Death. Differ. (2023).
[53] L Ai, A Xu, J Xu, Roles of PD-1/PD-L1 pathway: signaling, cancer, and beyond, Adv. Exp. Med. Biol. 1248 (2020) 33–59.
[54] M Yi, X Zheng, M Niu, S Zhu, H Ge, K Wu, Combination strategies with PD-1/PD-L1 blockade: current advances and future directions, Mol. Cancer 21 (1) (2022) 28.
[55] JH Cha, LC Chan, CW Li, JL Hsu, MC Hung, Mechanisms Controlling PD-L1 Expression in Cancer, Mol. Cell 76 (3) (2019) 359–370.
[56] Y Li, Z Wang, P Gao, D Cao, R Dong, M Zhu, Y Fei, X Zuo, J Cai, CircRHBDD1 promotes immune escape via IGF2BP2/PD-L1 signaling and acts as a nanotherapeutic target in gastric cancer, J. Transl. Med. 22 (1) (2024) 704.
[57] Y Luo, C Zeng, Z Ouyang, W Zhu, J Wang, Z Chen, C Xiao, G Wu, L Li, Y Qian, et al., YTH domain family protein 3 accelerates non-small cell lung cancer immune evasion through targeting CD8(+) T lymphocytes, Cell Death. Discov. 10 (1) (2024) 320.
[58] Q Chen, L Ao, Q Zhao, L Tang, Y Xiong, Y Yuan, X Wu, W Xing, Z Li, W Guo, et al., WTAP/YTHDF1-mediated m(6)A modification amplifies IFN-gamma-induced immunosuppressive properties of human MSCs, J. Adv. Res. (2024).
[59] Y Wang, P Jin, X Wang, N(6)-methyladenosine regulator YTHDF1 represses the CD8 + T cell-mediated antitumor immunity and ferroptosis in prostate cancer via m(6)A/PD-L1 manner, Apoptosis. 29 (1-2) (2024) 142–153.
[60] F Chen, Z Chen, T Guan, Y Zhou, L Ge, H Zhang, Y Wu, GM Jiang, W He, J Li, et al., N(6) -Methyladenosine Regulates mRNA stability and translation efficiency of krt7 to promote breast cancer lung metastasis, Cancer Res. 81 (11) (2021) 2847–2860.
[61] AA Shafi, AE Yen, NL Weigel, Androgen receptors in hormone-dependent and castration-resistant prostate cancer, Pharmacol. Ther. 140 (3) (2013) 223–238.
[62] MJ McAllister, MA Underwood, HY Leung, J Edwards, A review on the interactions between the tumor microenvironment and androgen receptor signaling in prostate cancer, Transl. Res. 206 (2019) 91–106.
[63] D Wang, C Cheng, X Chen, J Wang, K Liu, N Jing, P Xu, X Xi, Y Sun, Z Ji, et al., IL-1beta is an androgen-responsive target in macrophages for immunotherapy of prostate cancer, Adv. Sci. (Weinh) 10 (17) (2023) e2206889.
[64] P Xu, JC Yang, B Chen, C Nip, JE Van Dyke, X Zhang, HW Chen, CP Evans, WJ Murphy, C Liu, Androgen receptor blockade resistance with enzalutamide in prostate cancer results in immunosuppressive alterations in the tumor immune microenvironment, J. ImmunOther Cancer 11 (5) (2023).
[65] A Sun, Y Luo, W Xiao, Z Zhu, H Yan, C Miao, W Zhang, P Bai, C Liu, D Yang, et al., Androgen receptor transcriptionally inhibits programmed death ligand-1 expression and influences immune escape in bladder cancer, Lab. Invest. 103 (7) (2023) 100148.